JOURNAL OF MATERIALS SCIENCE 9 (1974) 1696–1700

X-ray topographic analysis of dislocations in Czochralski-grown stoichiometric $MgAl_2O_4$ spinel single crystals

E. KASPER
AEG-Telefunken Forschungsinstitut, 79 Ulm, Germany
P. KORCZAK, H. HENKEL
AEG-Telefunken Forschungsinstitut, 6 Frankfurt (Main) 71, Germany

Large stoichiometric $MgAl_2O_4$ spinel single crystals of high crystalline perfection have been grown by the Czochralski method. By means of X-ray diffraction topography the dislocation arrangement, Burgers vector directions and glide planes were investigated in relation to crystal growth conditions. Fast cooling rates generated prismatic dislocation hexagons in the central region of as-grown crystals. For the first time a new glide system in spinel following {311} planes was observed.

1. Introduction

Single crystal spinel $MgAl_2O_4$ has recently attracted interest as a transparent insulating substrate material for the hetero-epitaxial deposition of both silicon [1] and gallium arsenide [2] and potential use of such epitaxial semiconducting films in solid-state electronic devices. For this purpose large stoichiometric spinel single crystals with a high degree of crystalline perfection are required. However, up to now very little has been reported on the substructure and the dislocation arrangement of melt-grown stoichiometric spinel as revealed by X-ray diffraction topographic analysis [3].

The present work describes the results of X-ray topography of Czochralski-grown $MgAl_2O_4$ single crystals, especially their dislocation arrangement, Burgers vector directions and glide planes in relation to crystal growth conditions.

2. Experimental details

2.1. Crystal growth

Utilizing a standard Czochralski pulling system we have grown $MgAl_2O_4$ crystals from stoichiometric melts contained in inductively heated iridium crucibles. The component oxide powders MgO and Al_2O_3 (supplied by Merck and Koch-Light of quality 4N) were melted under inert nitrogen atmosphere. Transparent crystals up to 6 cm in length and 3 cm in diameter were grown on $\langle 111 \rangle$ seeds at pull and rotation rates within the range 2.5 to 5 mm h^{-1} and 10 to 50 rpm, respectively. The cooling rates of the as-grown crystals covered the range 10 to 50°C h^{-1}. The stoichiometric composition (MgO: Al_2O_3 = 1:1) of the crystals was confirmed by wet chemical analysis and a measured lattice parameter of 8.0849 ± 0.0003 Å. The latter, determined by X-ray Guinier diffraction technique is in good agreement with values already reported for stoichiometric spinel [3, 4].

2.2. X-ray topography

Thin (111) oriented spinel slices were cut perpendicular to the growth axis and on both sides subsequently mechanically polished to less than 150 μm thickness. In order to remove work damage introduced by mechanical polishing, which is detrimental to the topographic contrast [5], the specimens were further thinned by means of ion bombardment etching. Using argon ions at 2 kV and a current density of 70 μA cm^{-2}, approximately 2 μm thick surface layers were removed with a thinning rate of 1 μm h^{-1}. By this procedure topographic samples about 150 μm thick with improved surface quality were obtained (compare Fig. 1a and b).

Transmission and reflection topographs with $\{\bar{4}40\}$, $\{\bar{2}20\}$, $\{\bar{3}11\}$ and {333} type reflections were recorded with a standard Lang camera using Mo$K\alpha$ and Cu$K\alpha$ radiation. Absorption losses of Mo$K\alpha$ radiation in the examined thin spinel wafers were negligibly small ($\mu \cdot t = 0.2$,

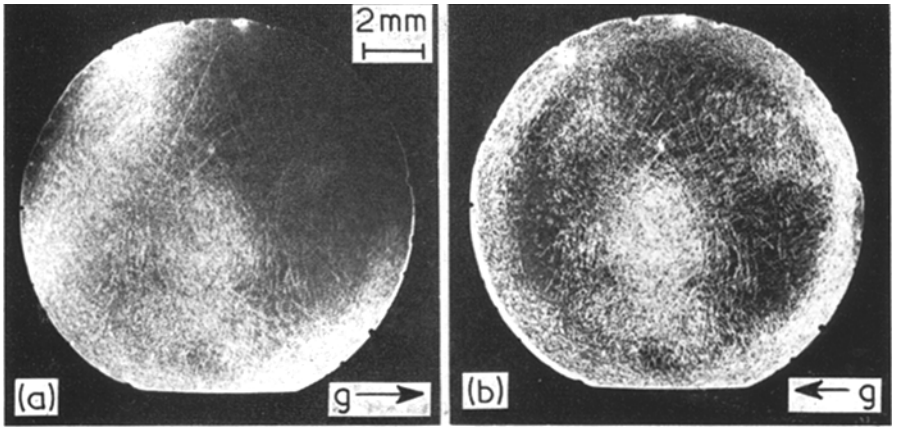

Figure 1 Topograph of slow cooled spinel (10°C h^{-1}), reflection $\{04\bar{4}\}$, with (a) only mechanical polishing (× 4); (b) additional ion bombardment etching (× 4).

where μ and t are the absorption coefficient and the thickness of the specimen) and therefore direct image contrast was dominant on the topographs.

3. Results and discussion

X-ray diffraction topography has been found to be useful to study lattice defects in low dislocation density crystals, especially the arrangement, Burgers vectors and glide planes of dislocations. In general Burgers vector analysis is based on the $(\mathbf{g} \cdot \boldsymbol{b})$ criterion, which predicts a contrast minimum on the topograph for $(\mathbf{g} \cdot \boldsymbol{b}) = 0$. The intensity of the contrast minimum is zero for a screw dislocation and is given by the product $\mathbf{g} \cdot (\boldsymbol{b} \times \mathbf{u})$ for an edge dislocation ($\mathbf{g}$ denotes the reciprocal lattice vector, $\boldsymbol{b}$ the Burgers vector and $\mathbf{u}$ the unit vector in dislocation direction).

For glide dislocations the Burgers vector and the dislocation lie within the glide plane. For dislocations generated by dislocation reaction or moved by climbing, the plane formed by vector $\boldsymbol{b}$ and $\mathbf{u}$ must necessarily not be a crystallographic possible glide plane. Therefore, an annealing experiment at 1850°C was carried out to study further the glide capability of different dislocation types.

3.1. Dislocation arrangement

In general it is confirmed by the X-ray diffraction topographs that our spinel crystals possess a high degree of crystalline perfection. The dislocation density, as revealed by etch pits typically several 10^3 cm^{-2}, is low enough to identify single dislocations on the topographs. In particular, low-angle boundary arrays and strained regions were not observed in ⟨111⟩ grown crystals, in agreement with an earlier publication by Cockayne *et al.* [3].

The general dislocation arrangement was not considerably influenced by variations of pull and rotation rates within the investigated ranges. However, different cooling rates applied to the as-grown crystals caused significant changes in the dislocation arrangement. The topographs of slowly cooled boules (10°C h^{-1}) exhibited three regions with different dislocation density (Fig. 1b). Central and marginal regions of crystal slices showed dense bundles of dislocations in contrast to the section in between. Such a distribution of dislocations was found to be typical for thermal strain caused by slow cooling of a cylindric crystal boule [6]. In contrast, fast cooled crystals (50°C h^{-1}) exhibited new structural defects in the central region, most of them recognized only as unresolveable longish spots, whereas marginal regions showed high density of dislocation bundles and none of the spot-like defects (Fig. 2).

3.2. Defects in fast cooled crystals

The larger hexagonal shaped structural defects in the central region of fast cooled crystals have been analysed in more detail. Stereographic topographs confirmed the observed defects to be scalene hexagons up to 120 μm in diameter located in (101) planes, which are inclined at 35° to the specimen surface (Fig. 3, E). Both parallel long edges of the hexagons lie in the

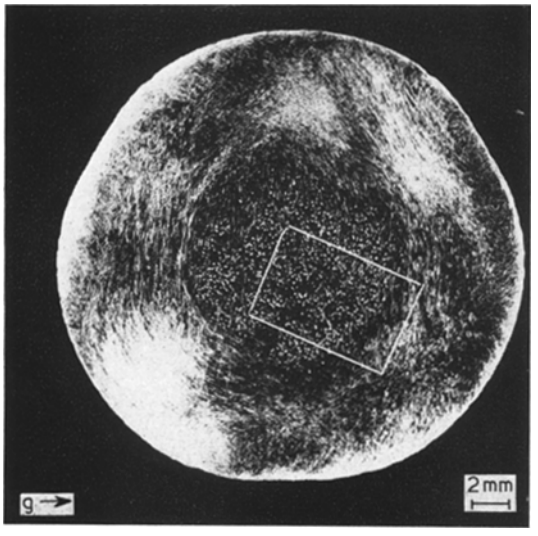

Figure 2 Topograph of fast cooled spinel (50°C h^{-1}), reflection $\{04\bar{4}\}$ (× 4).

[101] direction, the four shorter edges (approximately one third the length of the long edges) are nearly parallel to the $[12\bar{1}]$ and $[\bar{1}21]$ directions, respectively.

The observed topographic contrast behaviour of these defects is typical for prismatic dislocation hexagons. Contrast minimum for the hexagons in plane (101) was observed when the diffraction vector **g** was parallel to the long hexagon edges in direction $[10\bar{1}]$. In this case the long edges became invisible, only the connected short edges of the hexagons gave weak contrast reduced to the form of spots. Therefore, dislocation hexagons with the long edges parallel to **g** are revealed by an image of two spots (compare E in Figs. 3 and 4). On $(40\bar{4})$ topographs only defects with the long edges inclined 120° and 240°, to **g** are clearly visible as hexagons.

To calculate the contrast minimum, the Burgers vector, $\boldsymbol{b}$, was divided into two fractions lying within (α_s) and perpendicular (α_p) to the plane of the hexagon. Table I shows the different values of the criterion product $\mathbf{g} \cdot (\boldsymbol{b} \times \mathbf{u})$ for the long edges $[10\bar{1}]$ and the shorter edges $[12\bar{1}]$ and

TABLE I

u	$1/\sqrt{2}\ [10\bar{1}]$	$1/\sqrt{6}\ [12\bar{1}]$	$1/\sqrt{6}\ [\bar{1}21]$
$\mathbf{g} \cdot (\boldsymbol{b} \times \mathbf{u})$	0	1.63 α_p	1.63 α_p

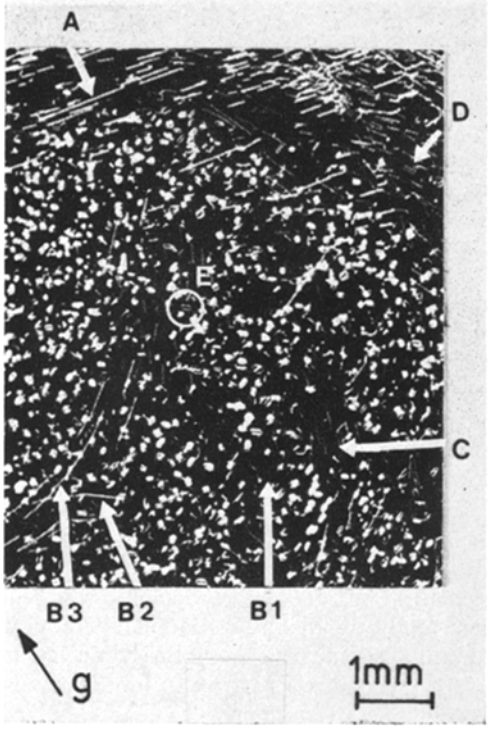

Figure 3 Enlarged view of central region of Fig. 2; $\mathbf{g} = \langle 04\bar{4} \rangle$, (× 10).

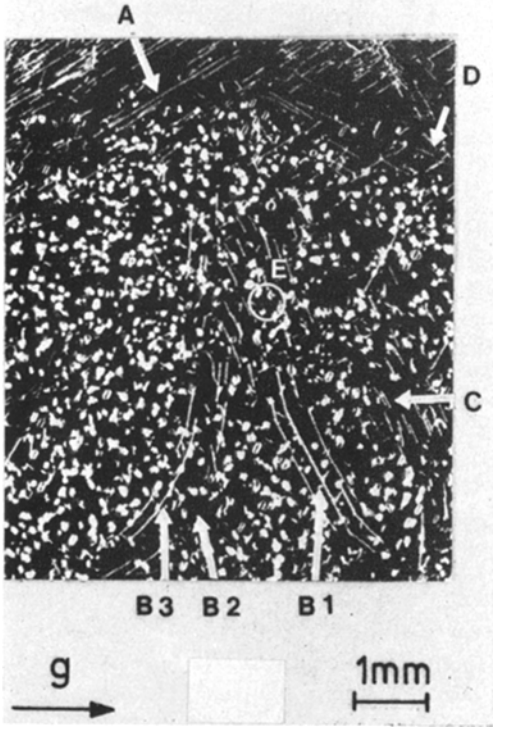

Figure 4 As Fig. 3, but $\mathbf{g} = \langle \bar{4}04 \rangle$, (× 10).

$[\bar{1}21]$ of the dislocation hexagons with $\mathbf{g} = \langle 10\bar{1}\rangle$ and $\boldsymbol{b} = \alpha_s \cdot [010] + \alpha_p \cdot [101]$. The shorter edges $[12\bar{1}]$ and $[\bar{1}21]$ can only cause intensity at the contrast minimum with $\mathbf{g} = [10\bar{1}]$ if $\alpha_p \neq 0$. Such a dislocation ring with a Burgers vector component perpendicular to the ring plane ($\alpha_p \neq 0$) is denoted as a prismatic dislocation ring.

3.3. Burgers vector analysis

From Hornstra [7] and Lewis [8] it is considered that in the spinel lattice a perfect dislocation has a $\frac{1}{2}\langle 110\rangle$ type Burgers vector. Therefore, a Burgers vector analysis with $\{4\bar{4}0\}$ and $\{\bar{3}11\}$ reflections was carried out under this assumption. The four types of dislocations mainly observed in our spinel crystals are indicated in Figs. 3, 4 and 5 by A, B, C and D. Directions, Burgers vectors and relevant angles between them are listed in Table II.

TABLE II

	Dislocation type			
	A	B	C	D
Direction	$\langle\bar{1}2\bar{1}\rangle$	$\langle 10\bar{1}\rangle$	$\langle\bar{1}12\rangle$	$\langle 001\rangle$
Burgers vector	$\frac{1}{2}\langle 10\bar{1}\rangle$	$\frac{1}{2}\langle 101\rangle$	$\frac{1}{2}\langle 0\bar{1}1\rangle$	$\frac{1}{2}\langle 1\bar{1}0\rangle$
Angle direction – Burgers vector	90°	90°	73°	90°

The angle between direction and Burgers vector is large for all of the investigated types of dislocations. Therefore, the dominant edge character of the dislocations is confirmed. According to the ($\mathbf{g} \cdot \boldsymbol{b}$) invisibility criterion, edge dislocations show extinction if $\mathbf{g}$ is parallel to the dislocation. In Figs. 3 and 4 the three possible directions (due to the three-fold symmetry of the $\langle 111\rangle$-axis) of B-type dislocations are indicated by B1, B2 and B3. From these figures it is evident that B1- and B2-type dislocations are invisible if they lie parallel to $\mathbf{g}$, corresponding to their edge characteristics.

3.4. Glide systems

To verify the dislocation glide mechanism an annealing experiment (1850°C for 4 h) was carried out. After crystal annealing, the dislocation hexagons and the A-type dislocations were unchanged (compare A and E in Figs. 4 and 5). B-type dislocations partially disappeared whereas C- and D-type dislocations completely

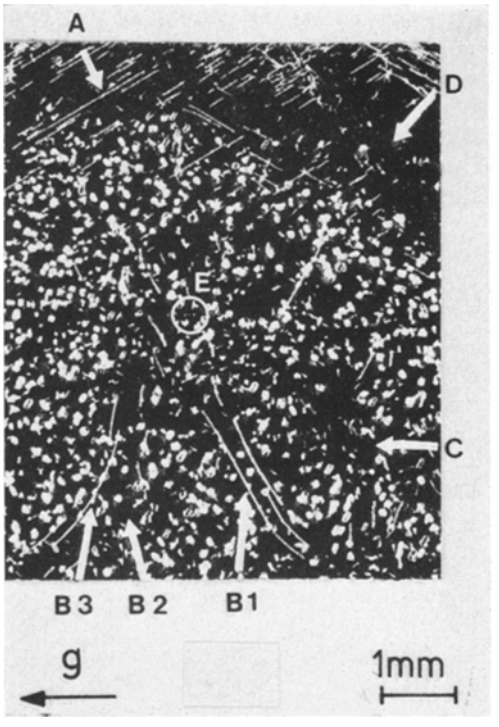

Figure 5 Topograph of fast cooled spinel after annealing (1850°C for 4 h), same crystal section as Fig. 4, (× 10).

vanished (compare C and D in Figs. 4 and 5.) Therefore, we assume that C- and D-type dislocations have changed their position by a glide process. It is very unlikely that these dislocations have moved by climbing so far that they could not be detected on the topographs.

The corresponding glide planes, calculated from directions and Burgers vectors of the dislocations, are $\{311\}$ for C-type and $\{110\}$ for D-type dislocations. $\{110\}$ glide planes already have been observed in non-stoichiometric spinel by Lewis [8], whereas $\{311\}$ glide planes in spinel here are reported for the first time.*

4. Conclusions

It has been observed that the dislocation arrangement of $\langle 111\rangle$ Czochralski-grown stoichiometric $MgAl_2O_4$ spinel single crystals is uninfluenced by variations of the growth parameters within the investigated ranges. In contrast, a clear dependence of the dislocation distribution on the crystal cooling procedure was found. For slow cooling rates (10°C h^{-1}) the dislocation arrangement is interpreted by thermal

*Previously, a metastable intermediate phase crystallizing in $\{311\}$ lamellae has been observed in connection with precipitations of Al_2O_3 in non-stoichiometric spinel [9].

strain generated during cooling of a cylindric crystal. Essentially edge dislocations were observed. At fast cooling rates (50°C h^{-1}) spinel crystals exhibited prismatic hexagons of dislocations in their central region.

From annealing experiments at 1850°C it is concluded that {110} and {311} are possible glide planes in spinel. The latter has been observed for the first time.

Acknowledgements

The authors wish to thank E. Fencl for helpful experimental assistance and D. Gruchmann and H. Kibbel for careful specimen surface preparation. They are also grateful to M. Gauntlett for lattice parameter measurements and to K. Post for providing wet chemical analysis.

References

1. G. W. CULLEN and F. C. DOUGHERTY, *J. Crystal Growth* **17** (1972) 230.
2. S. H. MCFARLANE and C. C. WANG, *J. Appl. Phys.* **43** (1972) 1724.
3. B. COCKAYNE, M. CHESSWAS, P. J. BORN and J. D. FILBY, *J. Mater. Sci.* **4** (1969) 236.
4. C. C. WANG and P. J. ZANZUCCHI, *J. Electrochem. Soc.* **118** (1971) 586.
5. J. E. A. MAURITS and A. M. HAWLEY, "Advances in X-ray Analysis" (edited by K. F. J. Heinrich *et al.*), (Plenum Press, New York, 1972) Vol. **15** p. 516.
6. P. PENNING, *Philips Res. Repts.* **13** (1958) 79.
7. J. HORNSTRA, *J. Phys. Chem. Sol.* **15** (1960) 311.
8. M. H. LEWIS, *Phil. Mag.* **17** (1968) 481.
9. H. SAALFELD and H. JAGODZINSKI, *Z. Krist.* **109** (1957) 87.

Received 23 April and accepted 13 May 1974.